Entropy-Scale Profiles for Texture Segmentation

Byung-Woo Hong, Kangyu Ni*, and Stefano Soatto

School of Computer Science and Engineering, Chung-Ang University, Seoul, Korea
School of Mathematical and Statistical Sciences, Arizona State University, USA
Computer Science Department, University of California, Los Angeles, CA, USA

Abstract. We propose a variational approach to unsupervised texture segmentation that depends on very few parameters and is robust to imaging conditions. First, the uneven illumination in the observed image is removed by the proposed image decomposition model that approximates the illumination and well retains the textures and features in the image. Then, from the obtained intrinsic image, we introduce a new data, multiscale local entropy, which is the entropy of each location's neighborhood histogram with various scales. The proposed segmentation model uses multiscale local entropy as data. Together with a length penalizing term, minimizing the energy functional locates the contours so that the local entropy within each region is similar to one another. Since entropy is the only feature, there are very few parameters. Moreover, the segmentation model can be solved by a fast global minimization method. Experimental results on natural images show the proposed method is able to robustly segment various texture patterns with uneven illumination in the original images.

1 Introduction

One of the challenges of unsupervised texture segmentation is due to the difficulties to well define textures. There are many tools to analyze texture, from statistical models to filtering methods, to geometric approaches. There have been a large number of texture features: orientations, scales, frequencies, etc. Therefore, partitioning an image domain into several texture regions, or identify homogeneous regions in the sense of texture, without any given knowledge is very difficult. One of the earliest unsupervised segmentation model [1] approximates an image by a piecewise smooth image and a length penalizing term in an energy functional to locate the boundary of each region. This model satisfies many desired mathematical properties but is difficult to solve in practice. In [2], the one-dimensional contour/edge set is approximated by a two-dimensional smooth function, making the functional easier to solve. The model in [3] approximates an image by a piecewise constant image and furthermore incorporates the level set method with the variational model, which makes it easy to solve. However, these classical methods do not handle textures, especially when the average intensities of each texture region are similar.

* Kangyu Ni was supported by the US NSF-DMS grant #0652833.

A.M. Bruckstein et al. (Eds.): SSVM 2011, LNCS 6667, pp. 243–254, 2012.

There has been numerous works on texture segmentation. For instance, the authors in [4], [5], and [6] use Gabor transforms to represent texture features for segmentations and authors in [7] use wavelet transforms. These generally have a large set of texture features and therefore involve selecting a large set of parameters. Probability density function (PDF)/ histogram-based approaches, such as [8], [9], [10], [11], and [12], also involve some parameters associated with the assumptions on the histograms or selected texture features. Methods in [13], [14], [15], [16], and [17] use the entire PDFs or histograms without extracting predefined features for segmentation using histogram distances, such as χ^2 statistics, mutual information, Kullback-Leibler divergence, and Bhattacharyya distance. The data of the histogram is not limited to intensity. Any features and transforms of the image can be used. However, finding the solutions of these methods requires differentiating histograms with respect to the contour or region. Local histogram-based methods [18] do not require histograms to be differentiated and can employ a fast global minimization method. However, the scale of the local histogram windows is fixed and has to be chosen. In this paper, we introduce a new data, multiscale local entropy, which is the entropy of a local neighborhood's histogram with various scales. Therefore, the window size is unbiased.

Another challenge of unsupervised texture segmentation is due to the imaging conditions/nuisance factors in real images. Most of the above-mentioned segmentation models are not robust to imaging conditions, because these are not taken into account in the segmentation models. The proposed segmentation model in [19] simultaneously estimates the illumination and reflectance and segments the image using reflectance. This allows global smooth changes within a region due to uneven lighting and is therefore robust with respect to nuisance factors. However, this model approximates images by piecewise constant functions and therefore does not handle textures. Note also the Mumford-Shah segmentation model, even though is difficult to solve, also deals with smooth changes in the image. However, it also does not handle textures.

For robust texture segmentation, we add a pre-processing step that approximately decomposes an image into an illuminance component and a reflectance component. The image model is described in section 2.1. The proposed decomposition model is described in section 2.2. For segmentation, we only use the reflectance component. In section 2.3, we proposed a new data for texture segmentation, multiscale local entropy. The segmentation model is described in section 2.4. Finally, we show some experimental results in section 3 and conclude in section 4.

2 Methodology

2.1 Image Model

The image of a natural scene captured by a camera does not solely depend on the objects in the scene. The lighting condition, or illumination, also plays an important role. Therefore, for robust image segmentation, illumination should be taken into account. Let $I : [0, 1] \times [0, 1] \to [0, 1]$ be the observed image after

normalization. One simple way to express the image with illumination is by the following multiplicative model:

$$I(x) = U(x)V(x), \tag{1}$$

where $x \in [0,1] \times [0,1]$, U is the illumination and V is the reflectance, or the intrinsic image structure. This model was formulated in [20] and was used for robust segmentation in [21] and [19]. Multiplicative noise model has been used for denoising and deblurring in [22] and segmentation in [23].

From this image model (1), we wish to find the reflectance component V and then use it for texture segmentation. To obtain V, we first take log of (1), which transforms the product model into the following sum:

$$\log I = \log U + \log V. \tag{2}$$

It is easier to decompose this additive expression than the multiplicative expression. In the next section, we provide a variational decomposition model for (2).

2.2 Image Decomposition

We take a variational PDE-based approach to decompose $\log I$. Let $f = \log I$, the decomposition is found by solving the following minimization problem:

$$\min_u \frac{1}{2} \int |\nabla u|^2 + \lambda \int |f - u|, \tag{3}$$

where λ is a parameter that controls the balance between the two penalty terms. The first term of the energy functional uses the ℓ_2 norm on the gradient of u because the illuminance component is approximately smooth. Note that more accurately the illumination is piecewise smooth, but the above approximation will suffice for the purpose of segmentation. The second term uses the ℓ_1 norm, rather than the ℓ_2 norm, on the residual, $f-u$, in order to better capture texture.

The solution of (3) can be found by using the gradient descent method:

$$\frac{du}{dt} = \triangle u + \lambda \frac{f-u}{|f-u|}, \tag{4}$$

where the parameter λ can be chosen by methods, such as in [24].

Figure 1 demonstrates this image decomposition method using several images from the Yale Face Database. The images, in row (a) from left to right, have lighting from different directions: center, right, and left, respectively. Row (b) shows the respective illumination components U, and row (c) shows the respective reflectance components V. For all three decompositions, the parameter $\lambda = 0.0004$. These experiments show the robustness of extracting the nuisance factors from the intrinsic image structure using the method described here. Specifically, the illumination components desirably exclude the image structure, and the reflectance components show uniform lighting on the faces. In addition, note that this decomposition model does not take into account shadows as part

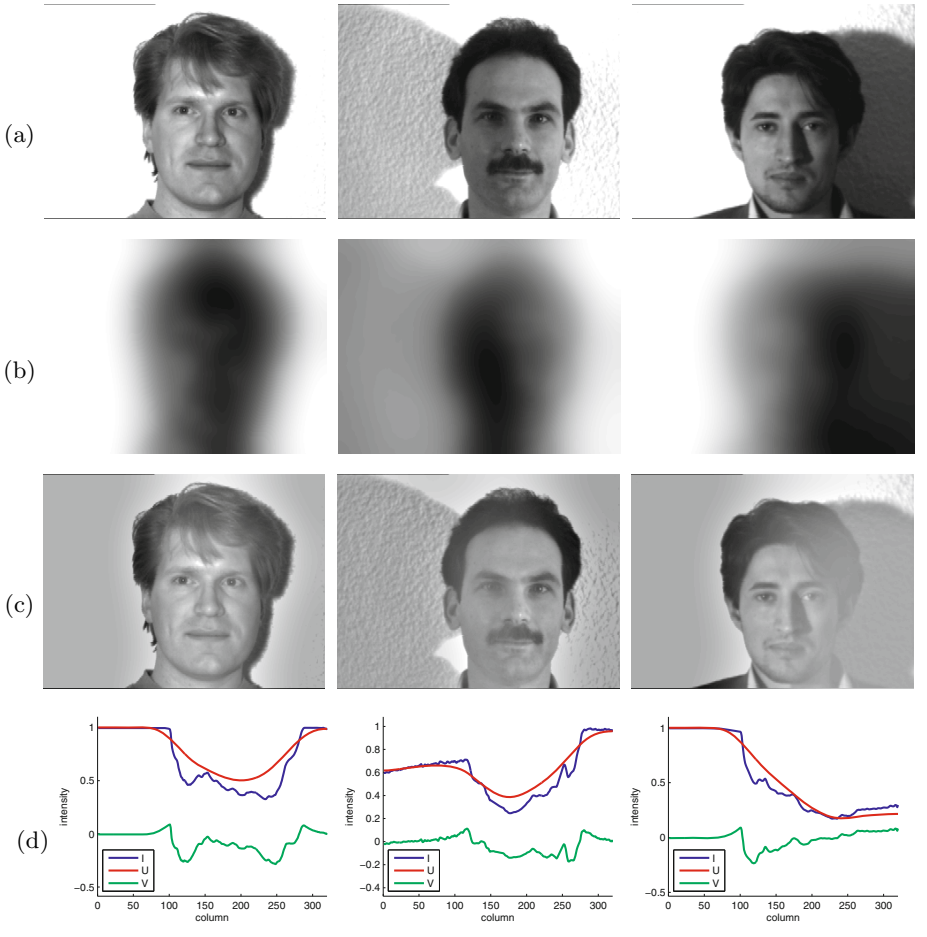

Fig. 1. Model (3) robustly decomposes images of faces with various lighting conditions into the illumination and intrinsic components. Row (a) shows original images I, row (b) shows illumination components U, row (c) shows reflectance components V, and row (d) shows vertical sum of intensity for each image

of illuminance and therefore is present in the reflectance component. Moreover, even though the areas with less lighting in the original images do not look as sharp in the reflectance image compared to the areas with more lighting originally, all areas possess similar levels of illuminance. This can also be seen in plots row (d), which shows the vertical sum of intensity for each original image, illumination, and reflectance components. For instance, since the lighting of the original image in the third row is from the left, we have high-left and low-right profile for the original image, high-left and low-right smooth profile for the illumination component, and more or less horizontal profile for the reflectance component.

2.3 Entropy Profile

In this section, we propose a descriptor that is calculated based on the reflectance component V and will be used for the proposed segmentation model described in the next section. First, let $h_{x,s}$ be the probability density function of image intensity on the square patch centered at location x with scale s. Note that in the discrete setting, the dimension of the patch is $(2s+1) \times (2s+1)$. Then, define $H_{x,s}$ as the entropy of $h_{x,s}$ by

$$H_{x,s} = -\int_0^1 h_{x,s}(y) \log(h_{x,s}(y))\, dy\ . \tag{5}$$

For a fixed location x, the entropy profile, $H_x(s)$, is a function of scale. In the following, we analyze the proposed entropy profile with a few examples..

Fig. 2 (a) is a synthetic image consisting of two textures with the same information (entropy) and different scales. The regions of each texture are indicated in (b). Four locations are selected in (c), and their respective entropy profiles are depicted in (e). Since both locations a and b are in the same texture region, their entropy profiles resemble each other. Similarly, the profiles of c and d resemble each other. In (f), the scale of entropy profile is adjusted by the logarithm, which is denoted by log-scale. Since entropy changes less as scale increases, entropy profiles in log-scale are more distinguishable. Figure (g) represents the median entropy profiles over all locations in each texture region, and (h) is the median entropy profiles in log-scale. The median entropy profiles are shown here because in the next section, the proposed segmentation model approximates the homogeneity of each region by using median entropy profile.

Fig. 3 illustrates with a synthetic image of two textures with the same scale and different information (entropy). Similarly, we see in (f) that the difference between profiles from different textures in log-scale is more prominent than without taking logarithms. Interestingly, the difference in entropy profiles in this case is in the vertical direction, instead of the horizontal direction in the previous example in Fig. 2. This is because the textures in Fig. 2 differ in scale and textures in Fig. 3 differ in information. However, if two textures have the same information and scale, the proposed entropy profile will not be able to distinguish them.

Fig. 4 shows a different perspective of entropy using a real image. Instead of looking at a entropy profile $H_x(s)$, which is a function of scale with a fixed location, each image is an entropy map $H_s(x)$, which is defined as the entropy of each location with a fixed scale. The scales are from 1 to 24, from left to right and top to bottom. Each row shares the same color bar at the end of the row, where dark red represents the highest value and dark blue represents the lowest value. The entropy maps change quickly when the scales are small, as shown in the first row, and do not change very much when the scales are large, as shown in the third and fourth rows. Therefore, for segmentation, we use log-scale for the scale in entropy maps.

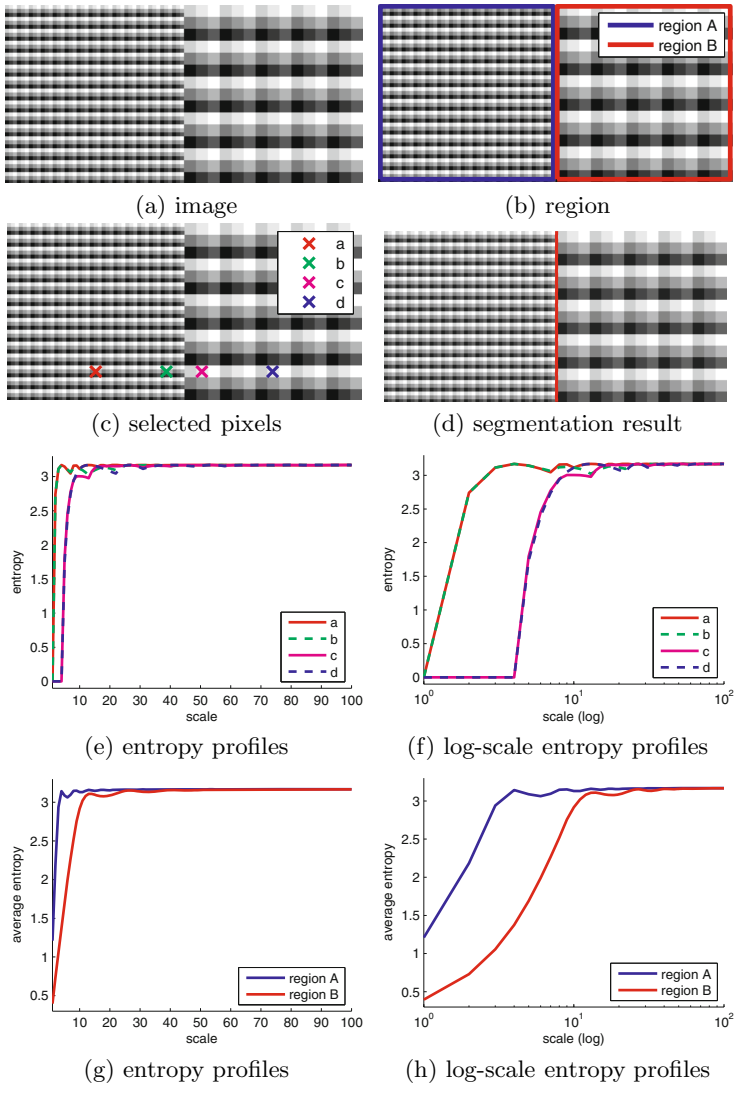

(a) image (b) region

(c) selected pixels (d) segmentation result

(e) entropy profiles (f) log-scale entropy profiles

(g) entropy profiles (h) log-scale entropy profiles

Fig. 2. The entropy profiles $H_x(s)$ of textures with same information and different scales are distinct

2.4 Texture Segmentation

The proposed texture segmentation model uses the entropy profile $H_x(s)$ of the reflectance component V in

$$\min_{u,H_1,H_2} \int |\nabla u(x)|\, dx + \lambda \int u(x)\; d(H_1, H_x) + [1 - u(x)]\;\; d(H_2, H_x)\; dx\;, \quad (6)$$

where $0 \leq u \leq 1$, H_1 and H_2 are unknown histograms, λ is a parameter, and the distance between two histograms is defined as

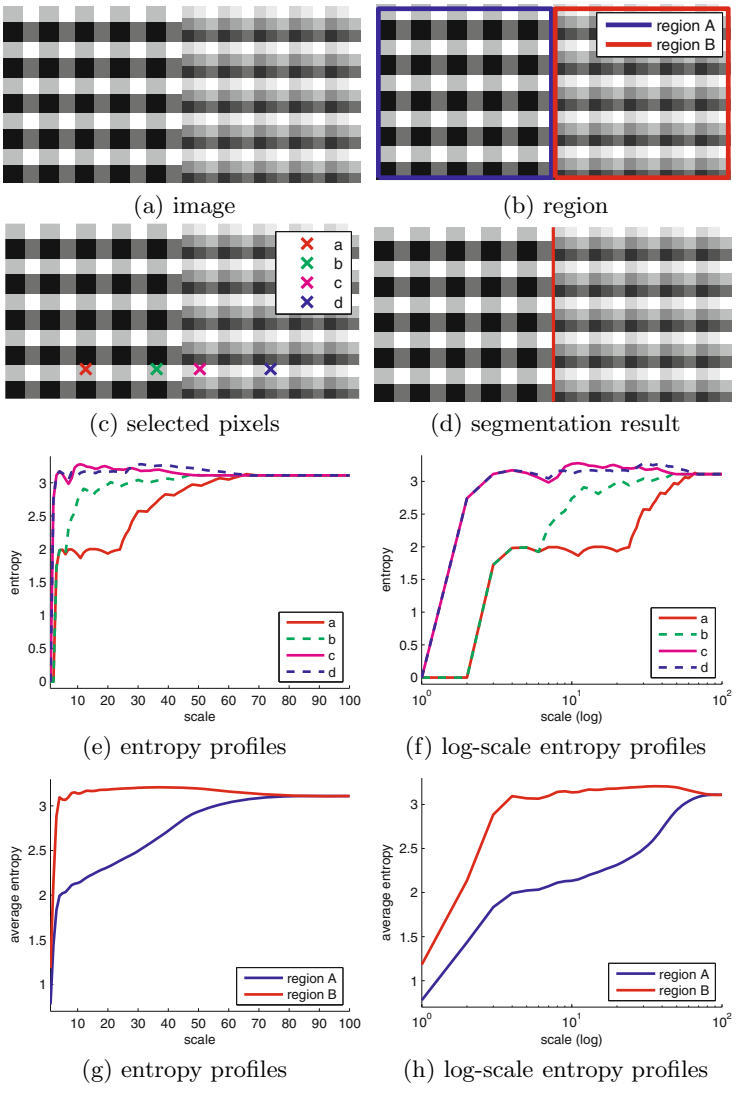

(a) image (b) region

(c) selected pixels (d) segmentation result

(e) entropy profiles (f) log-scale entropy profiles

(g) entropy profiles (h) log-scale entropy profiles

Fig. 3. The entropy profiles $H_x(s)$ of textures with same scale and different information are distinct

$$d(H_1, H_x) = \int |H_1(s) - H_x(s)| \ \log(s)\, ds, \tag{7}$$

which incorporates log-scale. The variable u represents the segmented regions. The set of u close to 1 is inside the contour and the set of u close to 0 is outside the contour. According to [25], minimizing this energy functional with respect to u is a convex problem. The data terms encourage finding contours so that the local entropy profiles are similar to one another within each region. The proposed segmentation model (6) resembles the local histogram based segmentation model

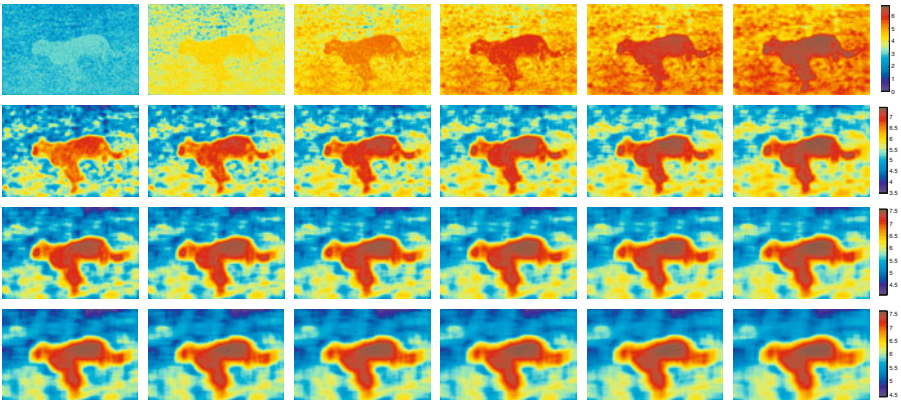

Fig. 4. Entropy maps $H_s(x)$ of the center image in Fig. 5 (a) with scale from 1 to 24, from left to right and top to bottom. The difference in maps becomes small when the scale increases.

with the Wasserstein distance in [18]. Nevertheless, it is in essence different, since entropy profile takes into account of various scales, rather than using a fixed-size window. As a result, this segmentation is more robust than local histogram-based methods, whose patch size needs to be close to the texture scale in the image.

To solve (6), we may follow the fast global minimization method described in [18] and [26]. Therefore, without repeating the derivations, the minimization is solved by repeating the following steps until convergence:

$$H_1(s) = \text{weighted (by } u(x)) \text{ median of } H_x(s) \tag{8}$$

$$H_2(s) = \text{weighted (by } 1-u(x)) \text{ median of } H_x(s) \tag{9}$$

$$\overrightarrow{p}(x) = \frac{\overrightarrow{p}(x) + \delta t \, \nabla(\operatorname{div}\overrightarrow{p}(x) - v(x)/\theta)}{1 + \delta t \, |(\operatorname{div}\overrightarrow{p}(x) - v(x)/\theta)|} \tag{10}$$

$$u(x) = v(x) - \theta \operatorname{div}\overrightarrow{p}(x) \tag{11}$$

$$v(x) = \max\{\min\{u(x) - \theta\lambda r_{x,H_1,H_2}, 1\}, 0\}, \tag{12}$$

where θ is a parameter, δt is a time-step that is $\leq \frac{1}{8}(\delta x)^2$, $\overrightarrow{p}(x) = (p_1(x), p_2(x))$, and

$$r_{x,H_1,H_2} = \int |H_1(s) - H_x(s)| - |H_2(s) - H_x(s)| \, ds.$$

The initializations can be arbitrary since this is a global minimization model. Therefore, one may initially choose an arbitrary contour and let $u = 1$ inside the contour and $u = 0$ outside the contour. Initializations for v and $\overrightarrow{p}$ can be done by setting $v = u$ and $\overrightarrow{p} = \overrightarrow{0}$.

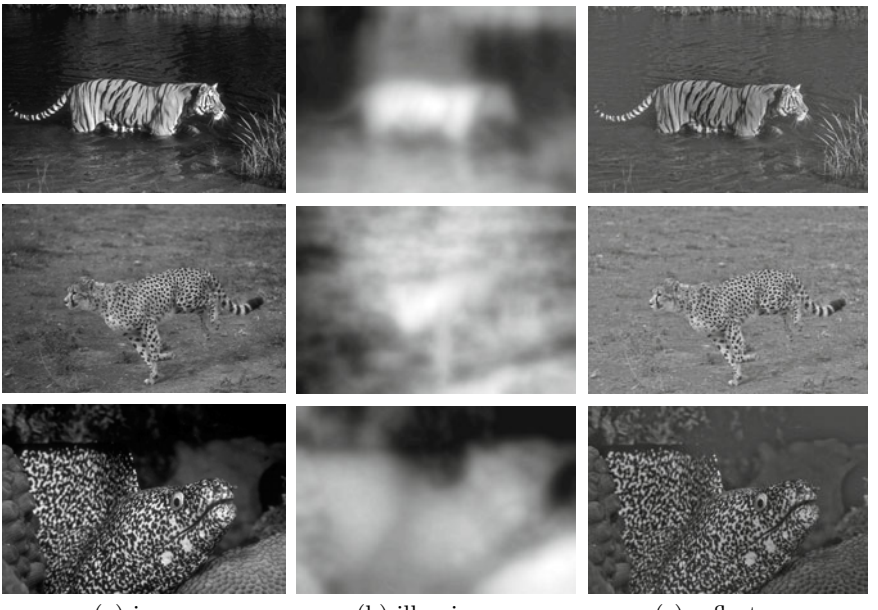

(a) image (b) illuminance (c) reflectance

Fig. 5. Model (3) robustly decomposes real images from Berkeley segmentation database. The reflectance components appear to have even lighting.

Fig. 2 (d) and fig. 3 (d) show the segmentation model (6) is able to accurately distinguish two textures, in which one pair of textures has the same information but different scales and the other pair has the same scale but different informations.

3 Experimental Results

Fig. 5 evaluates the proposed decomposition model with a few images from the Berkeley segmentation database, as shown in column (a). Their respective illuminance components U are shown in column (b), and the reflectance components V are shown in column (c). The illuminance appears to be faithfully extracted. As one can see, for instance, the front of the cheetah body is more illuminated than other areas in the original image. The left side of the background is less illuminated than other areas in the original image. Therefore, the reflectance in (c) desirably looks flat because the lighting is forced to be homogeneous. Similar observations can be made for the other two images.

Fig. 6 shows segmentation results using the proposed model (6) and other methods for the purpose of comparison. Row (b) shows segmentation results using the fast global minimization of active contour (GAC) in [26], which approximates an image by a piecewise constant function and therefore performs poorly for images with rich texture patterns. Rows (c) and (d) show segmentation

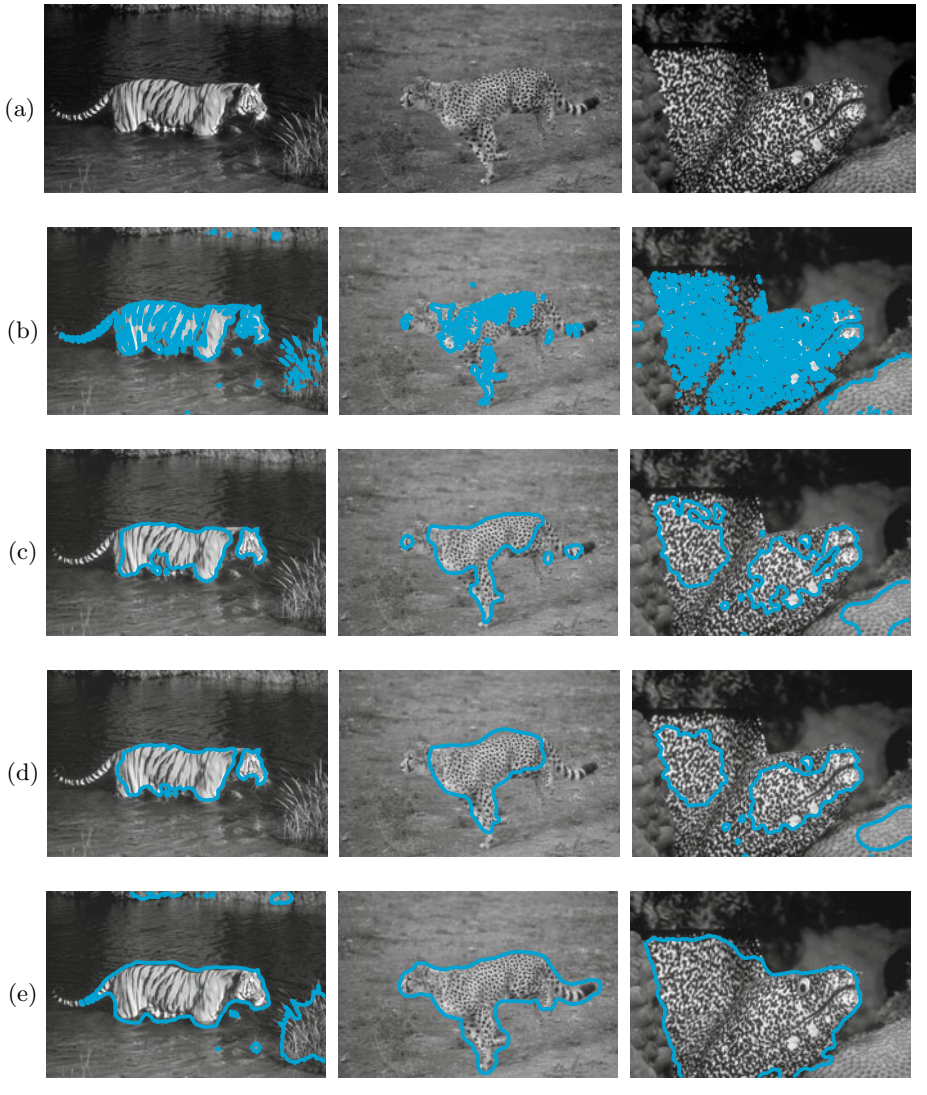

Fig. 6. (a) are the original images. (b) are the segmentation results by the fast global minimization of active contour (GAC) in [26]. (c) are the results by local histogram based segmentation using the Wasserstein distance (LHSWD) [18] with scale = 10. (d) are the results by LHSWD with scale = 30. (e) are the results by the proposed method, which is more robust to illumination than GAC and LHSWD and is able to segment the texture patterns more accurately.

results by the local histogram based segmentation method using the Wasserstein distance (LHSWD) in [18]. For the local histograms, the binning size is 100 and the scale sizes are 10 and 30 for (c) and (d), respectively. The parameters are $\theta = 0.001$ and $\lambda = 1$. Row (e) shows results of the proposed method with the

same parameters θ and λ. The results are far better as one can see that the patterns of tiger, cheetah, and fish are more accurately segmented. We believe that this is due to two reasons. First, illuminance in an image plays an important role in segmentation, and it is to beneficial to even out the illuminance. Second, all scales of local histograms were taken into account, rather than using a fixed scale.

4 Conclusion

We propose a method for texture segmentation that is robust to imaging conditions using very few parameters. We propose a multiscale local entropy as a data descriptor and an image decomposition model for illumination removal. While it is possible to put the decomposition and segmentation models in one formulation, it is in practice difficult to solve. Therefore, the decomposition is done as a pre-processing step. The experimental results show that the proposed method is able to accurately segment natural images that contain texture patterns. In the future, we would like to analyze and extend the use of entropy profile.

Acknowledgments. This work was supported by the Korea Research Foundation Grant funded by the Korean Government (NRF-2010-220-D00078).

References

1. Mumford, D., Shah, J.: Optimal approximations by piecewise smooth functions and associated variational problems. Comm. Pure Appl. Math. 42(5), 577–685 (1989)
2. Ambrosio, L., Tortorelli, V.M.: Approximation of functionals depending on jumps by elliptic functionals via gamma convergence. Comm. on Pure and Applied Math. 43, 999–1036 (1990)
3. Chan, T., Vese, L.A.: Active contours without edges. IEEE Trans. on Image Processing 10(2), 266–277 (2001)
4. Jain, A.K., Farrakhonia, F.: Unsupervised texture segmentation using gabor filters. Pattern Recognition 23(12), 1167–1186 (1991)
5. Chan, T., Sandberg, B., Vese, L.: Active contours without edges for textured images. UCLA Comput. Appl. Math. Rep. 02-39 (2002)
6. Sagiv, C., Sochen, N.A., Zeevi, Y.Y.: Integrated active contours for texture segmentation. IEEE Transactions on Image Processing 15(6), 1633–1646 (2006)
7. Portilla, J., Simoncelli, E.P.: A parametric texture model based on joint statistics of complex wavelet coefficients. International Journal of Computer Vision 40(1)
8. Manjunath, B.S., Chellappa, R.: Unsupervised texture segmentation using markov random field models. IEEE Transactions on Pattern Analysis and Machine Intelligence 13(5), 478–482 (1991)
9. Zhu, S.C., Yuille, A.: Region competition: Unifying snakes, region growing, and bayes/mdl for multiband image segmentation. IEEE Trans. on Pattern Analysis and Machine Intelligence 18(9), 884–900 (1996)
10. Yezzi, J.A., Tsai, A., Willsky, A.: A statistical approach to snakes for bimodal and trimodal imagery. In: Int. Conf. on Computer Vision, pp. 898–903 (1999)

11. Paragios, N., Deriche, R.: Geodesic active regions and level set methods for supervised texture segmentation. International Journal of Computer Vision 46(3)
12. Rousson, M., Brox, T., Deriche, R.: Active unsupervised texture segmentation on a diffusion based feature space. In: Computer Vision and Pattern Recognition
13. Aubert, G., Barlaud, M., Faugeras, O., Jehan-Besson, S.: Image segmentation using active contours: Calculus of variations or shape gradients? SIAM Appl. Math. 1(2), 2128–2145 (2003)
14. Herbulot, A., Jehan-Besson, S., Duffner, S., Barlaud, M., Aubert, G.: Segmentation of vectorial image features using shape gradients and information measures. J. Math. Imaging and Vision 25(3), 365–386 (2006)
15. Kim, J., Fisher, J.W., Yezzi, A., Cetin, M., Willsky, A.S.: A nonparametric statistical method for image segmentation using information theory and curve evolution. IEEE Trans. on Image Processing 14, 1486–1502 (2005)
16. Awate, S.P., Tasdizen, T., Whitaker, R.T.: Unsupervised texture segmentation with nonparametric neighborhood statistics. In: Leonardis, A., Bischof, H., Pinz, A. (eds.) ECCV 2006. LNCS, vol. 3952, pp. 494–507. Springer, Heidelberg (2006)
17. Michailovich, O., Rathi, Y., Tannenbaum, A.: Image segmentation using active contours driven by the bhattacharya gradient flow. IEEE Trans. on Image Processing 16(11), 2787–2801 (2007)
18. Ni, K., Bresson, X., Chan, T., Esedoglu, S.: Local histogram based segmentation using the wasserstein distance. International Journal of Computer Vision 84(1), 97–111 (2009)
19. Li, C., Li, F., Kao, C.-Y., Xu, C.: IImage Segmentation with Simultaneous Illumination and Reflectance Estimation: An Energy Minimization Approach. In: Proc. of ICCV (2009)
20. Horn, B.K.P.: Robot Vision. MIT Press, Cambridge (1986)
21. Chen, T., Yin, W., Zhou, X.S., Comaniciu, D., Huang, T.S.: Total variation models for variable lighting face recognition. IEEE Trans. on Pattern Analysis and Machine Intelligence 28(9), 1519–1524 (2006)
22. Rudin, L., Lions, L., Osher, S.: Multiplicative denoising and deblurring: theory and algorithms, vol. 445. Springer, Heidelberg (2003)
23. Le, T.M., Vese, L.A.: Additive and Multiplicative piecewise-smooth segmentation models in a functional minimization approach. Contemporary Mathematics (2007)
24. Aujol, J.F., Gilboa, G., Chan, T., Osher, S.: Structure-texture image decomposition - modeling, algorithms, and parameter selection. International Journal of Computer Vision 67(1), 111–136 (2006)
25. Chan, T., Esedoglu, S., Nikolova, M.: Algorithms for finding global minimizers of image segmentation and denoising models. SIAM Journal on Applied Mathematics 66(5), 1632–1648 (2006)
26. Bresson, X., Esedoglu, S., Vandergheynst, P., Thiran, J.P., Osher, S.: Fast global minimization of the active contour/snake model. Journal of Mathematical Imaging and Vision 28(2), 151–167 (2007)